Electronic Supplementary Information (ESI)

Solution structure of thrombin binding aptamer complex with a non-planar platinum(II) compound

Bo-Chen Zhu,[#a] Juan He,[#b] Xiao-Yu Xia,[#a] Jingxing Jiang,[c] Wenting Liu,*[a] Liu-Yi Liu,[a] Bing-Bing Liang,[a] Hua-Gang Yao,[b] Zhuofeng Ke,*[c] Wei Xia,*[a] Zong-Wan Mao*[a]

[a] *MOE Key Laboratory of Bioinorganic and Synthetic Chemistry, School of Chemistry, Sun Yat-Sen University, Guangzhou 510275, China*

[b] *School of Pharmaceutical and Chemical Engineering, Guangdong Pharmaceutical University, Zhongshan 528458, China*

[c] *School of Materials Science and Engineering, PCFM Lab, School of Chemistry, Sun Yat-sen University, Guangzhou 510275, China.*

** To whom correspondence should be addressed. Wenting Liu (Email: liuwenting@mail.sysu.edu.cn); Zhoufeng Ke (Email: kezhf3@mail.sysu.edu.cn); Wei Xia (Email: xiawei5@mail.sysu.edu.cn); Zong-Wan Mao (Email: cesmzw@mail.sysu.edu.cn).*

[#] *These authors contributed equally to this work.*

MATERIAL AND METHODS

Materials and instruments

The materials used in this study were obtained from the following sources. The organic raw materials and solvent for synthesis were all purchased from Alfa Aesar and the platinum ligand for synthesis was purchased from Shanghai Libo. All the DNA oligonucleotides were synthesized by Sangon Biotech (Shanghai) Co., Ltd. The thrombin and fibrinogen were purchased from Sigma-Aldrich. PPACK was purchased from GlpBio. Human serum was purchased from Future. FRET assay was performed on a Light Cycler II real-time PCR (Roche, Switzerland). CD data were collected on a JACSO J-1600 spectrophotometer (JASCO, Japan). Orbitrap Fusion Lumos Tribrid Mass Spectrometer (Thermo Fisher Scientific, Germany) was used in ESI-MS. Bruker AVIII 600 MHz/700 MHz spectrometer equipped with a cryoprobe (Bruker, USA) was used in NMR experiments. MicroCal ITC200 (Malvern, England) was used in ITC experiments.

Synthesis and characterization of L'$_2$LPt

Synthesis of N-methyl-(N'-2-pyridine) imidazol-N'-ium chloride (L'Cl)[1] (Scheme S1, Step 1): 2.28 g (20.0 mmol) of 2-chloropyridine (Alfa Aesar) and 1.64 g (20.0 mmol) of 1-methylimidazole (Alfa Aesar) were weighed and mixed in a dry reaction tube, sealed by N_2 and reacted at 160 ℃ for 48 h. The product was cooled to obtain a dark brown oily liquid and precipitated several times by $CHCl_3$/Et_2O to give a brown oily liquid which was dried in vacuo. Weighed: 2.20 g, Yield: 56%.

Synthesis of dichloride-bridged platinum precursor [LPt(Cl)$_2$PtL][2] (Scheme S1, Step 2): 1.2 mM (0.5 g) dipotassium tetrachloroplatinate (Shanghai Libo) is added under nitrogen protection to 5 mL of deionized water, then 1.2 mM (0.23 g) 2-(2,4-difluorophenyl) pyridine (L) dissolved in 15 mL of 2-ethoxyethyl ether (Alfa Aesar) was added and the mixture was heated to 80 ℃ for 48 h. The mixture was cooled and a large amount of ice-cold water was added to obtain yellow chloroform precipitate. The product was filtered, washed with ethanol and then dried in vacuo. Weighed: 0.58 g. Yield: 62%.

Synthesis and characterization of L'$_2$LPt complex (Scheme S1, Step 3): 0.38 g (0.5 mmol) of chlorine-bridged platinum precursor and 0.28 g (1.2 mmol) of carbene ligand were added into a dry flask and dissolved in 15 mL of CH_2Cl_2 and 1.5 mL triethylamine. The solution was protected by nitrogen and kept at 70 ℃ for 28 h. After solvent removal by evaporation, the reaction mixture was purified by silica gel column chromatography. The final product was eluted by petroleum ether-dichloromethane-triethylamine. Regular yellow-green crystals were obtained using slow evaporation method with dichloromethane /anhydrous ethanol as solvent. Weighed: 0.28 g. Yield: 20%.

The ligand and final organometallic complex were characterized by ^{1}H, ^{13}C NMR (Bruker AVIII 600 MHz spectrometer) and ESI-MS (Thermo LTQ XL) (Supplementary Figure S1-S3).

Oligonucleotides

All the DNA oligonucleotides were purchased from Sangon Biotech (Shanghai) Co., Ltd. The oligonucleotides for circular dichroism (CD), polyacrylamide gel electrophoresis (PAGE) and nuclear magnetic resonance (NMR) were purified by ultra-polyacrylamide gel electrophoresis (ULTRAPAGE); the oligonucleotides for ESI-MS were purified by high performance liquid chromatography (HPLC) and the oligonucleotides for FRET assay were labelled by fluorescent groups FAM at the 5'-end and TAMRA at the 3'-end (FAM: 6-carboxyfluorescein, TAMRA: 6-carboxytetramethylrhodamine) and purified by HPLC. G4 DNA was folded by heating the dissolved oligonucleotides to 95 ℃ for 5 min followed by cooling to room temperature overnight. The concentrations of DNAs were measured by Nanodrop 200/200c (Thermo Scientific, USA).

Fluorescence resonance energy transfer (FRET) melting assay

The oligonucleotides labelled by FAM and TAMRA were dissolved in deionized water to prepare stock solutions with a final concentration of 50 μM. The stock solution was diluted with 10 mM Tris-HCl buffer containing 60 mM potassium cacodylate (pH 7.4) and then subjected to annealing. Stock solution of L'$_2$LPt (10 mM) was diluted to 100 μM using the same buffer. FRET thermal melting assay was performed on a Light Cycler II real-time PCR (Roche, Switzerland) with 25 μL reaction samples containing 0.40 μM labelled oligonucleotide and the same equivalent of L'$_2$LPt. The excitation and detection wavelengths were 470 nm and 530 nm, respectively. The fluorescence readings were recorded at intervals of 1 ^{o}C over the temperature range of 37-99 ^{o}C, with a constant temperature being maintained for 30 s prior to data collection to ensure a stable value. Final data analysis was carried out using Origin 9.0 software (OriginLab Corp., USA).

The FRET experiments using buffers with different K^+ concentrations were conducted to make different DNA FRET melting temperature in the 63 ± 2 ℃ interval. The K^+ concentrations used for each different DNA is shown in Table S5.

For competitive FRET experiments, all of the conditions of the reaction system were similar to the FRET assay. except different equivalent (0:1, 1:1, 15:1, 50:1) of different kinds of DNAs (ds26, VEGF, Tel26, HIV-PRO1) were added in the L'$_2$LPt and FAM/TAMRA labeled TBA FRET thermal melting system. The ratio of L'$_2$LPt combined with TBA in the competitive environment is calculated by the following formula:

$$R_{Pt-TBA} = \frac{T_{m(Pt/TBA)} - T_{m(Pt/TBA)comp}}{T_{m(Pt/TBA)} - T_{m(TBA)}} \quad (1)$$

where $R_{Pt\text{-}TBA}$ is the ratio of L'$_2$LPt combined with TBA in the competitive environment. $T_{m(Pt/TBA)}$ is the FRET melting temperature of 1:1 L'$_2$LPt/TBA complex. $T_{m(Pt/TBA)comp}$ is the FRET melting temperature of 1:1 L'$_2$LPt/TBA complex in competitive environment. $T_{m(TBA)}$ is the FRET melting temperature of free TBA G4.

Circular dichroism (CD) titration and melting assay

CD experiments were performed on a JACSO J-1600 spectrophotometer (JASCO, Japan) equipped with a Peltier temperature controller using a quartz cuvette with a path length of 1 cm. The DNA oligonucleotide was dissolved and annealed in Tris-HCl (10 mM, pH 7.4) buffer supplemented with 100 mM KCl to a final concentration of 3.0 μM.

In CD titration assay, different amounts of L'$_2$LPt complex were titrated into TBA solution followed by equilibrium for 3 min at ambient temperature prior to data collection. CD spectra were recorded from 225 to 500 nm in a step of 1 nm at a scan rate of 200 nm/min. Then a cycle of heating and cooling with the temperature changing rate 30 ℃/h after each ligand addition. The CD spectral intensity variation with temperature data was collected at 295 nm. The Three scans were averaged for each spectrum. Data analysis was carried out using Origin 9.0 (OriginLab Corp., USA).

In CD melting assay, CD spectra of different DNA and the same equivalent of L'$_2$LPt with DNA complex were recorded to find out the characteristic peaks of each DDNA. CD melting studies were carried out between 25-100 ℃ with the heating rate 30 ℃/h at highest CD characteristic peaks of each DNA. Data analysis was carried out using Origin 9.0 (OriginLab Corp., USA).

Ultraviolet–Visible (UV/Vis) titration assay

UV/Vis titration experiments were performed on a Cary 100 UV/Vis spectrophotometer (Agilent, USA) using a 3 mL quartz cuvette with a path length of 1 cm. The DNA oligonucleotide was dissolved and annealed in Tris-HCl (10 mM, pH 7.4) buffer supplemented with 100 mM KCl to a final concentration of 500.0 μM. Stock solution of L'$_2$LPt (10 mM) was diluted to 20 μM using the same buffer. The Tris-HCl (10 mM, pH 7.4) buffer supplemented with 100 mM KCl was also used in the reference pool. TBA G4 DNA were titrated into L'$_2$LPt solution and reference pool in 0.2 molar ratios each time. The UV/vis titration spectra were recorded from 290 to 450 nm. Data analysis was carried out using Origin 9.0 (OriginLab Corp., USA).

Negative Electrospray Ionization Mass Spectrometry (ESI-MS)

For ESI-MS, TBA G4 DNA stock solution was diluted in 150 mM ammonium acetate buffer (pH 7.4) to a final concentration of 10.0 μM. Different molar equivalents (0.5, 1.0, 1.5, 2.0, 3.0) of L'$_2$LPt were titrated and the mixture was incubated at ambient temperature for 1 h before MS data collection. The ESI-MS spectra was performed on an Orbitrap Fusion Lumos Tribrid Mass Spectrometer (Thermo Fisher Scientific, Germany). Data analysis was performed as previous reports[3, 4]. The apparent DNA binding constant (K_{app}) value was determined by the peak areas of the 4^- charge state of free TBA G4 and TBA G4 bound with L'$_2$LPt, assuming that the response factors are equal for all the species. The relative areas of the mass spectral peaks were extracted using MassLynx 4.0 (Waters, USA). The equilibrium of L'$_2$LPt-TBA G4 were calculated as following equation:

$$K_{app} = [L'_2LPt\text{-}TBA]/[L'_2LPt][TBA] \quad (2)$$

The curves of L'$_2$LPt versus TBA G4 concentrations were fitted using the DynaFit software[5] to obtain K_{app} values. The DynaFit software approximates the K_{app} values to fit the concentrations of the input stoichiometries as a function of total ligand added. These inputs are the concentrations of each L'$_2$LPt-TBA species obtained by MS (0 L'$_2$LPt and 1 L'$_2$LPt) and the output consist of the K_{app} values and the corresponding fits.

Isothermal titration calorimetry (ITC)

ITC experiments were performed on a MicroCal ITC200 (Malvern, England). The thrombin (Sigma-Aldrich)

was purified as described previously.[6, 7] In brief, 6 μM thrombin together with the same equivalent of PPACK inhibitor (D-Phe-Pro-Arg-chloromethylketone) (GlpBio) was dissolved and dialyzed against 10 mM Tris-HCl buffer supplemented with 100 mM KCl (pH = 7.4). The TBA G4 were also dissolved and annealed in the same buffer. To exclude the effect of DMSO dilution in PBS buffer, the same amount of DMSO were added into the solution in syringe and cell. Each solution was degassed by vacuum aspiration for 5 min at room temperature prior to loading the samples in the ITC cell and syringe. Typically, all titrations were carried out at 25 ℃ with a stirring speed of 600 rpm and a 120 s duration between each 2 μL injection titrated into 280 μL. All ITC data were analysed using the Microcal Origin version 7.0 software package. Dissociation constants were calculated by fitting the data to one-set binding model. Thermodynamic parameters N (stoichiometry), K_a (association constant) and ΔH (enthalpy change) were obtained by nonlinear least-squares fitting of experimental data using a one-set binding model in binary system and competitive binding model in ternary system provided with the instrument. Each ITC experiments were repeated at least twice for each condition.

NMR experiments

NMR data were collected on the Bruker AVIII 600 MHz or AVIII 700 MHz spectrometer equipped with a cryoprobe. 0.15-1.0 mM sample was prepared in a solution of 25 mM K-phosphate and 70 mM KCl buffer at pH 7.0, 90% H_2O/10% D_2O. Assignments of the TBA–L'$_2$LPt complex were accomplished using a combination of homonuclear 2D NMR experiments including DQF-COSY, TOCSY and NOESY. The mixing times were set from 50-300 ms for NOESY, and 20-100 ms for TOCSY. WATERGATE or pre-saturation water suppression techniques were applied for samples in water solution. Peak assignments and integrations were achieved using Topspin (Bruker, Germany) and Sparky (UCSF, USA).

NOE-distance restrained molecular dynamics simulation

The distances between protons were calculated based on the nuclear overhauser effect (NOE) cross-peaks integrated in NOESY spectra. The upper and lower boundaries were set to ± 20% for the estimated distances. The distance between Me-H6 in thymine (2.99 Å) was set as a reference [8]. The 1:1 L'$_2$LPt–TBA G4 complex structure calculations were performed in the program X-PLOR [9] and Accelrys Discovery Studio 2.5.5. The L'$_2$LPt molecule was geometry optimized and calculated the partial atomic charges by b3lyp/lanl2dz using the Gaussian 09 (Table S1). The Dynamic simulation and NOE-restrained simulation annealing calculations were performed as described before [8] by using Accelrys Discovery Studio and X-PLOR. The best 10 structures were selected based on the minimum energy and number of NOE violations.

Fibrinogen clotting assay

The fibrinogen clotting assay was performed as previously described [10]. Different concentrations of TBA (0, 200, 500, 1000 nM) with or without L'$_2$LPt, $TMPyP_4$ and PDS were incubated for 5 min at 37.0 ℃ in PBS supplemented with 2.0 mg/ml of fibrinogen (Sigma-Aldrich) in a PMMA cuvette (vol 1.0 ml, cell length 1.0 cm; ThermoFisher). 100 μl thrombin (1 NIH/ml; Sigma-Aldrich) was then added into the fibrinogen solution mixture. The time required for fibrin polymerization was determined based on the UV absorbance at 380 nm. The experiments were performed in triplicate for each concentration. The clotting time value reported as mean ± SE was derived as the maximum of the second derivative of each scattering curve.

Supplementary Scheme

Step 1: N_2, 160 ℃, 48h.

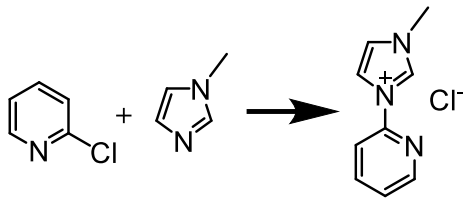

Step 2: N_2, 80 ℃, 48h.

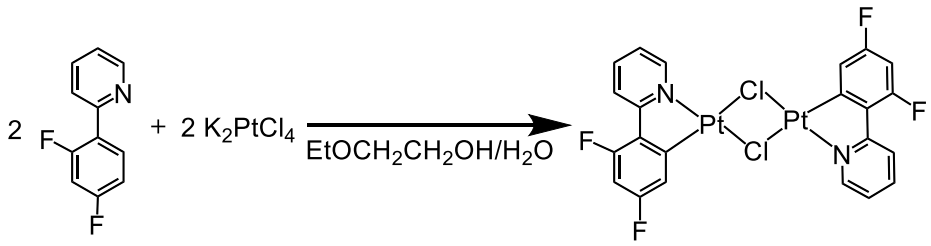

Step3: ①N_2, 70 ℃, 28h.

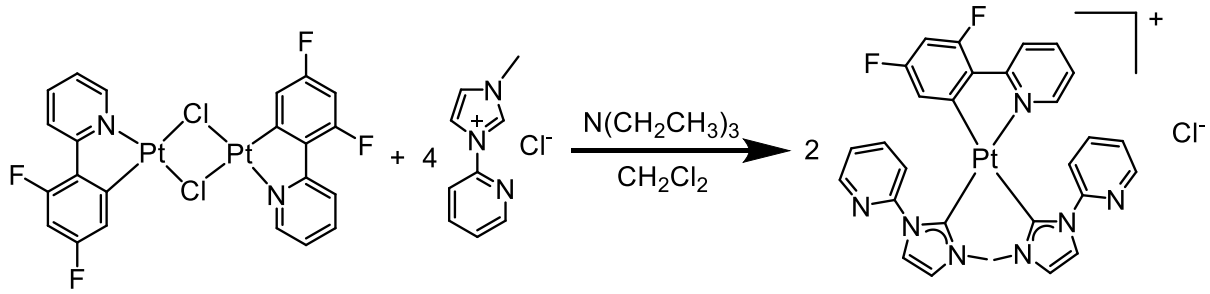

Scheme S1. Synthetic route to L'$_2$LPt.

Supplementary Figures

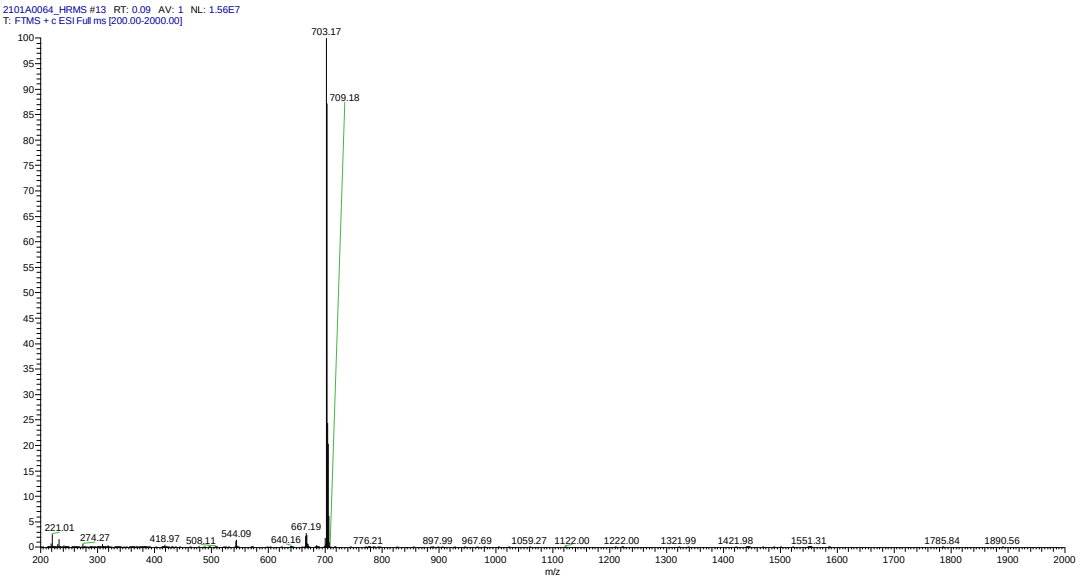

Fig. S1 MS spectrum (Thermo LTQ XL) of L'$_2$LPt. The m/z calcd for L'$_2$LPt: 703.17 (703.17, 100%; 704.17, 82.2%; 702.17, 73.3%); found: 703.17.

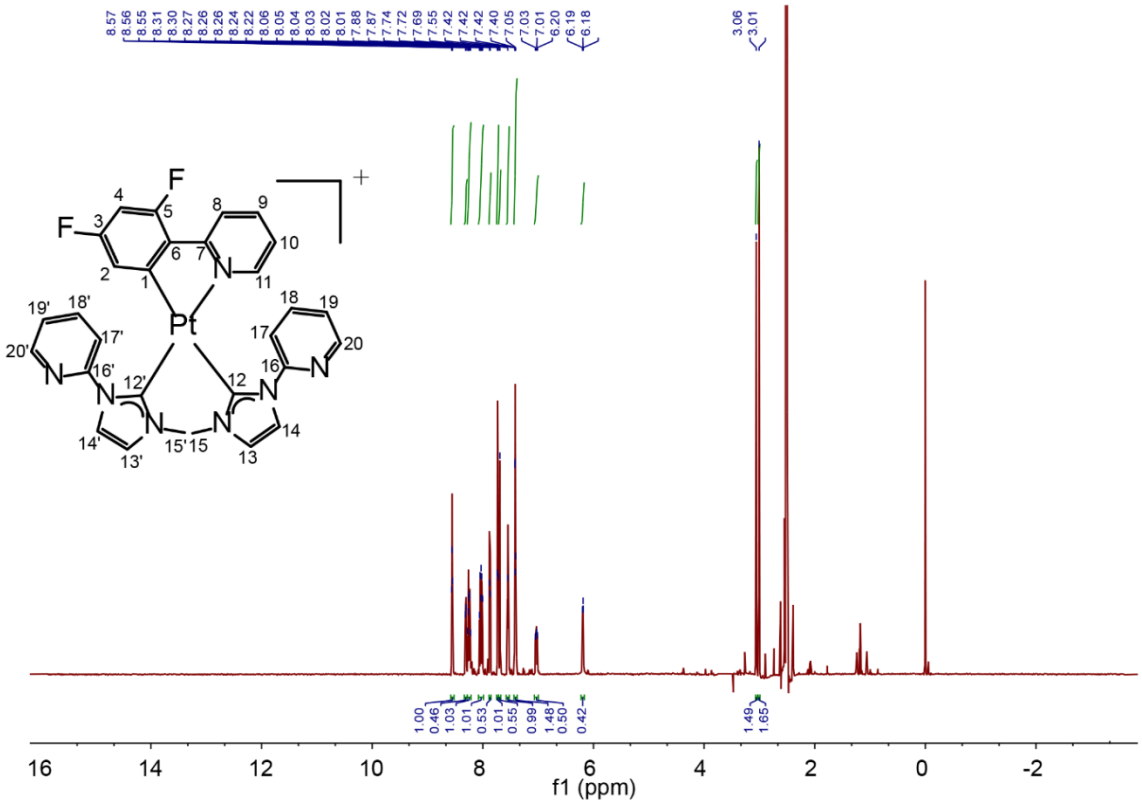

Fig. S2 ^{1}H NMR spectrum of L'$_2$LPt. (Bruker AVIII 600 MHz spectrometer, DMSO-d_6, 298 K): δ H20/H20' 8.57-8.55 (dtd, J = 4.7, 1.9, 0.8 Hz, 2H), H13/H13', H11 8.31 - 8.22 (m, 3H), H17/H17' 8.05-8.01 (dtd, J = 11.7, 7.7, 1.9 Hz, 2H), H8 7.88-7.87 (dt, J = 8.1, 1.0 Hz, 1H), H19/H19' 7.74 - 7.69 (m, 2H), H18/H18' 7.55 (ddt, J = 7.5, 4.9, 1.2 Hz, 2H), H14/H14', H10 7.42 - 7.40 (m, 3H), H4 7.05-7.01 (ddd, J = 12.9, 9.2, 2.4 Hz, 1H), H2 6.20-6.18 (dd, J = 8.0, 2.4 Hz, 1H), Me15' 3.06 (s, 3H), Me15' 3.01 (s, 3H).

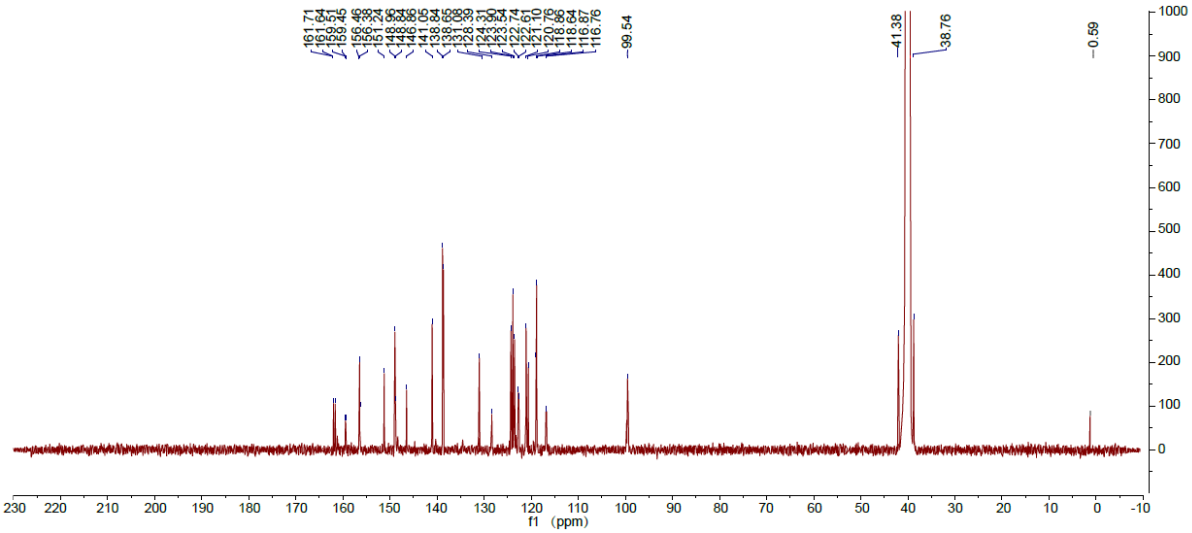

Fig. S3 ^{13}C NMR spectrum of L'$_2$LPt. (Bruker AVIII 600 MHz spectrometer, DMSO-d_6, 298 K): δ C3 161.71, C5 161.64, C16 159.51, C16' 159.45, C18 156.46, C18' 156.38, C7 151.24, C20 148.96, C20' 148.84, C11 146.86, C7 141.05, C12 138.84, C12' 138.65, C1 131.08, C6 128.39, C8 124.31, C19 123.90, C19' 123.54, C13 122.74, C13' 122.61, C10 121.10, C2 120.76, C14 118.86, C14' 118.64, C17 116.87, C17' 116.76, C4 99.54, C15 41.38, C15' 38.76.

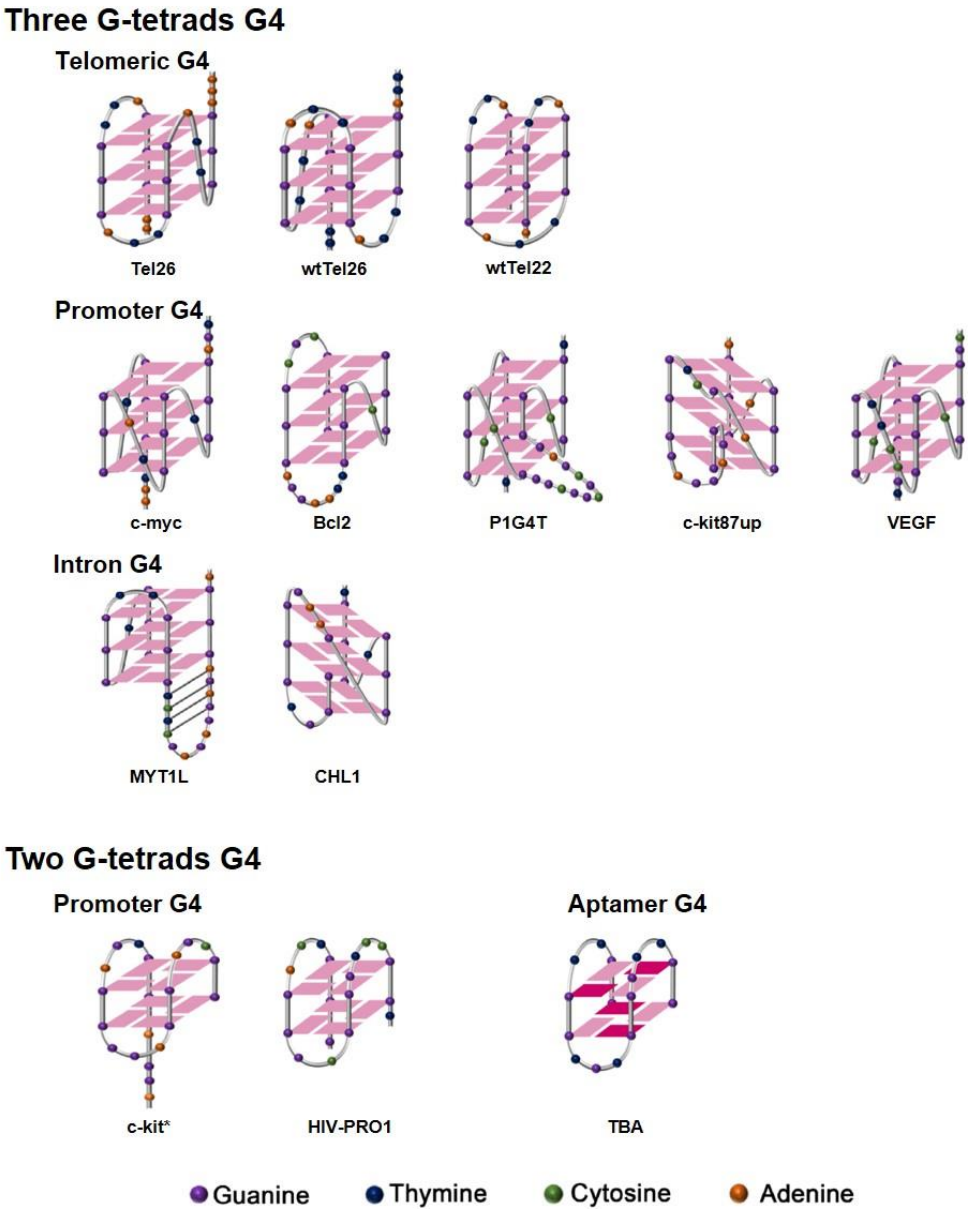

Fig. S4 The folding topology of G-quadruplexes (G4s) used in the FRET and CD-melting assay.

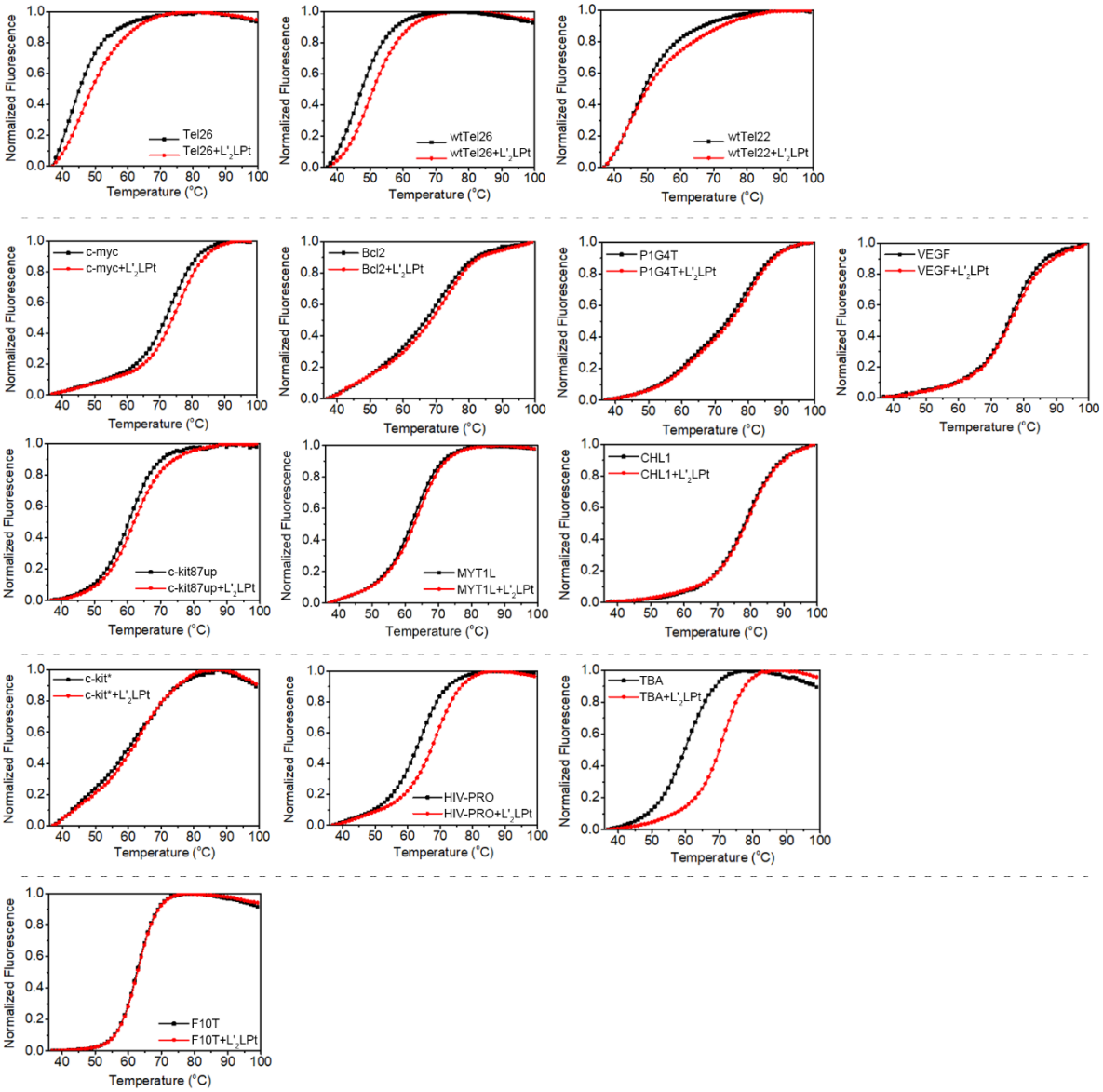

Fig. S5 FRET-melting curves of different G4s and duplex DNA at a concentration of 0.40 μM interacting with 0.40 μM L'$_2$LPt in 10 mM Tris-HCl buffer (pH 7.4) containing 60 mM potassium cacodylate.

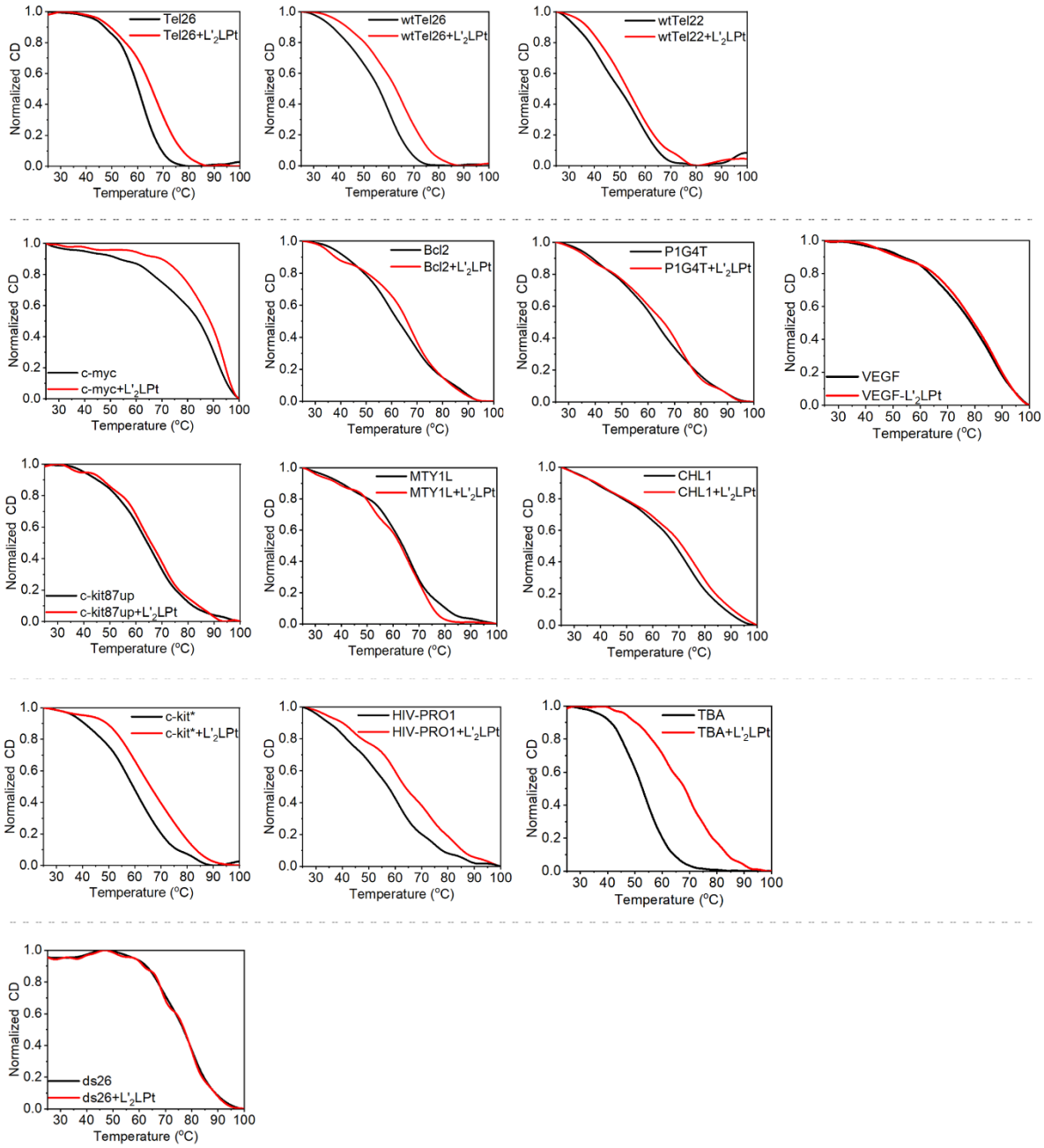

Fig. S6 CD-melting curves of different G4s and duplex DNA in 10 mM Tris-HCl, 100 mM KCl buffer (pH 7.4).

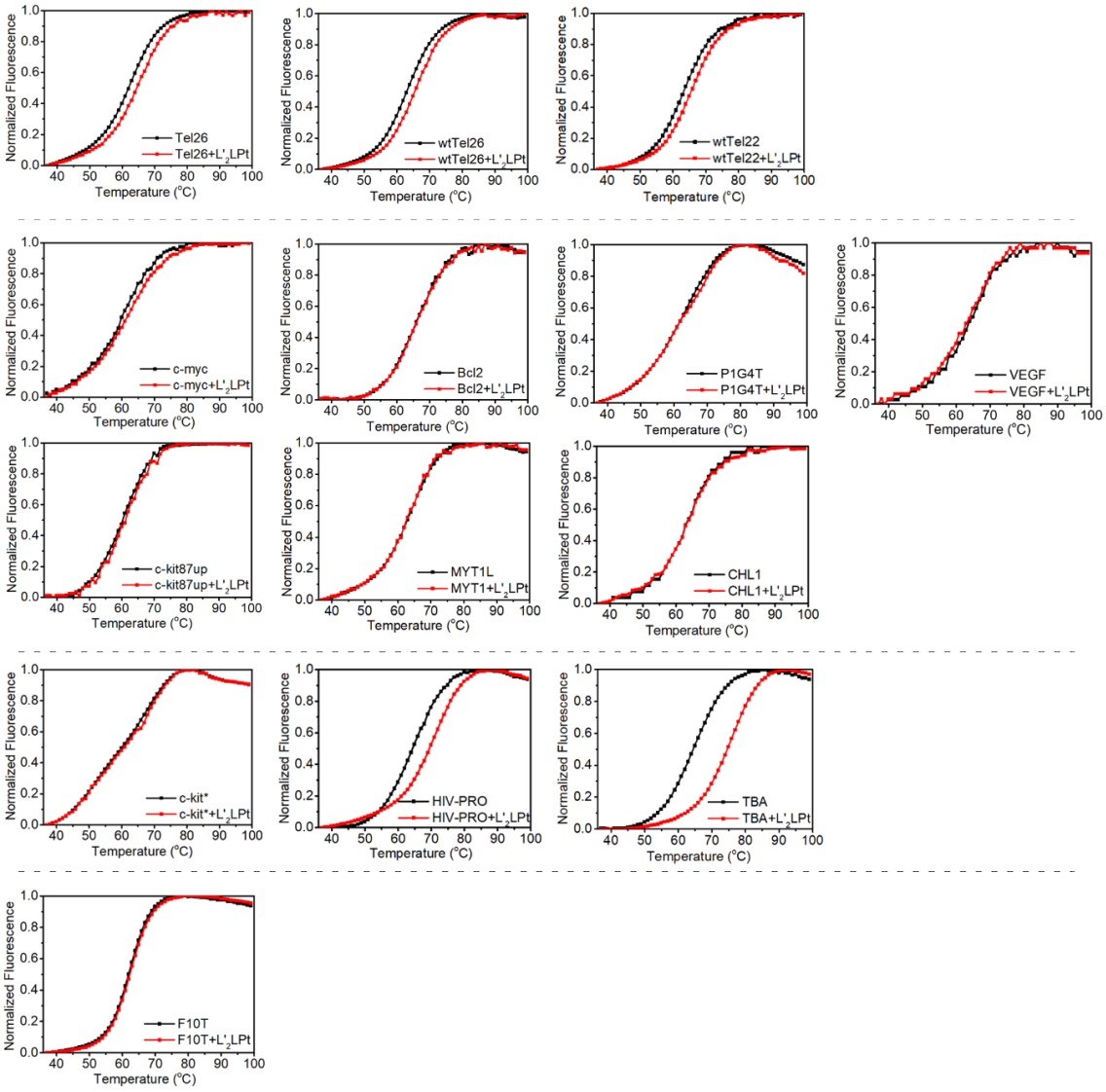

Fig. S7 FRET-melting curves of different G4s and duplex DNA at a concentration of 0.40 μM interacting with 0.40 μM L'$_2$LPt in 10 mM Tris-HCl buffer (pH 7.4) containing different concentration of K+ to make each DNA Tm value in the 63 ± 2 ℃ interval.

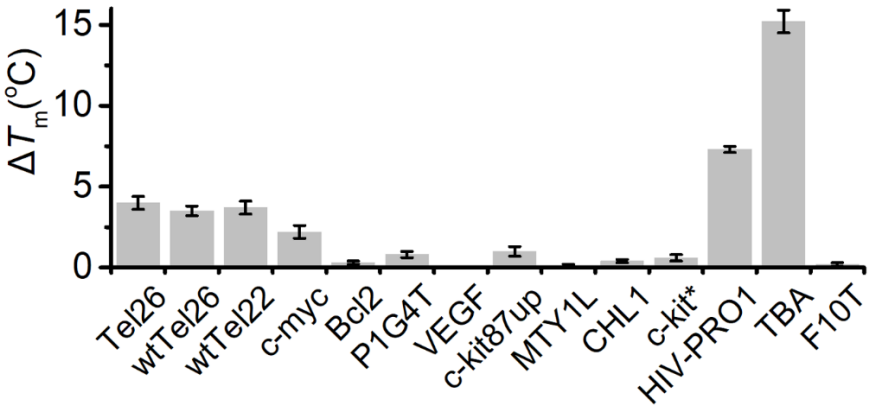

Fig. S8 FRET ΔT_m value of different G4s and duplex DNA. FRET data were tested in a concentration of 0.40 μM DNA interacting with 0.40 μM L'$_2$LPt in 10 mM Tris-HCl buffer (pH 7.4) containing different concentration of K^+ to make each DNA T_m value in the 63 ± 2 ℃ interval.

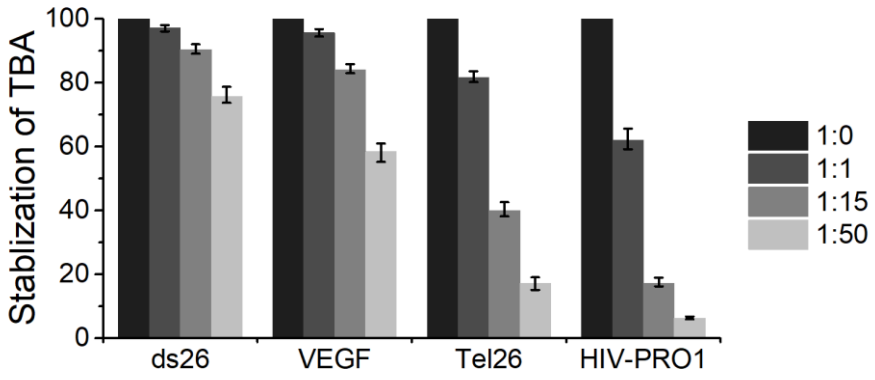

Fig. S9 FRET competition experiments with different ratios (1:0, 1:1, 1:15, 1:50) of duplex-DNA and G4 (ds26, VEGF, Tel26, HIV-PRO1) added to TBA. Conditions:10 mM Tris-HCl buffer containing 60 mM potassium cacodylate, pH = 7.4.

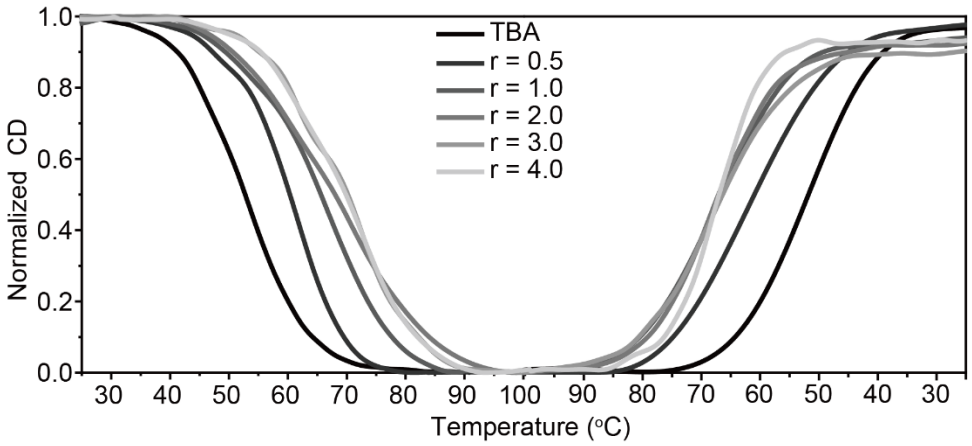

Fig. S10 CD melting spectra tested from 25 ℃ to 100 ℃ and cool down to 25 ℃ of L'$_2$LPt titrated into TBA G4 DNA solution at different L'$_2$LPt/TBA ratios. Conditions: pH 7.4, 10 mM Tris-HCl, 100 mM KCl solution.

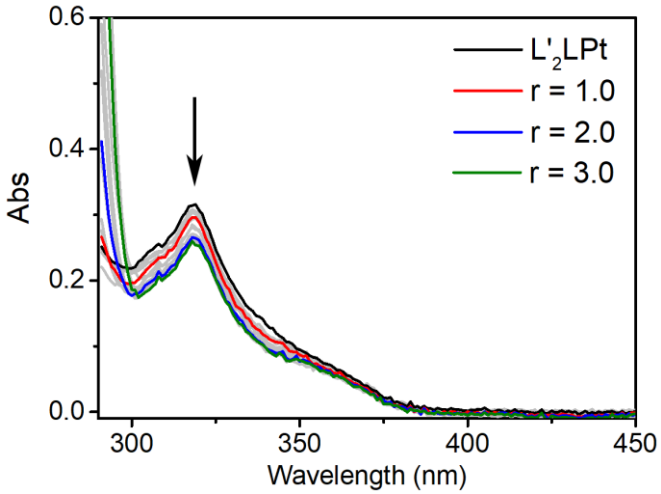

Fig. S11 UV/vis spectra of TBA G4 DNA titrated into L'$_2$LPt solution in 0.2 molar ratios each time. Non-integer molar ratio spectra are represented in gray, and integer ratio spectra are represented in different colors as shown in the figure. Conditions: pH 7.4, 10 mM Tris-HCl, 100 mM KCl solution.

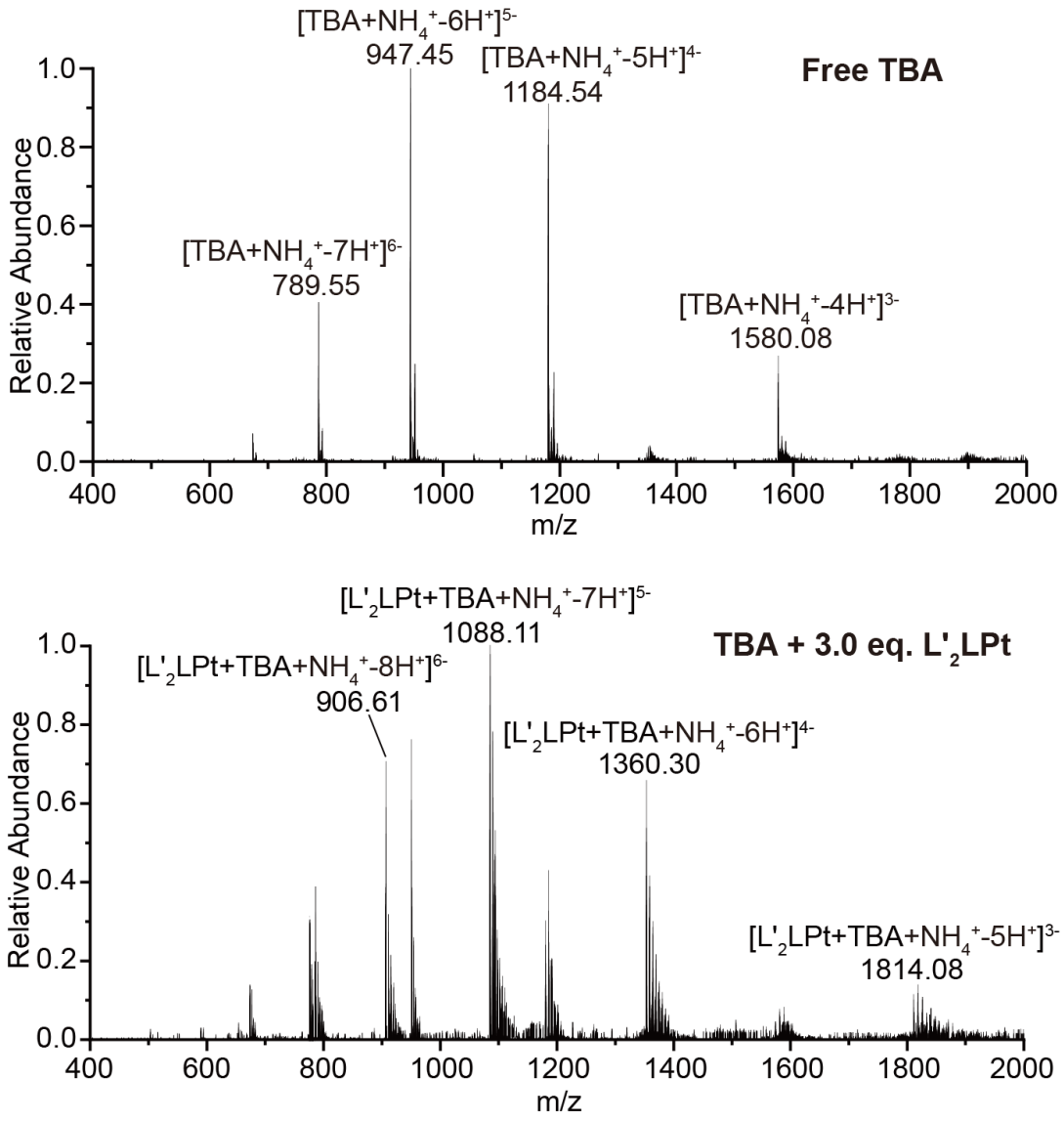

Fig. S12 ESI-MS spectra of the free TBA G4 and the TBA G4 interacting with L'$_2$LPt at 3.0 L'$_2$LPt/TBA ratio. The ion peaks for free TBA G4 and the 1:1 L'$_2$LPt–TBA G4 complex are labelled. Conditions: pH 7.4, 150 mM ammonium acetate ($CH_3CO_2NH_4$) buffer.

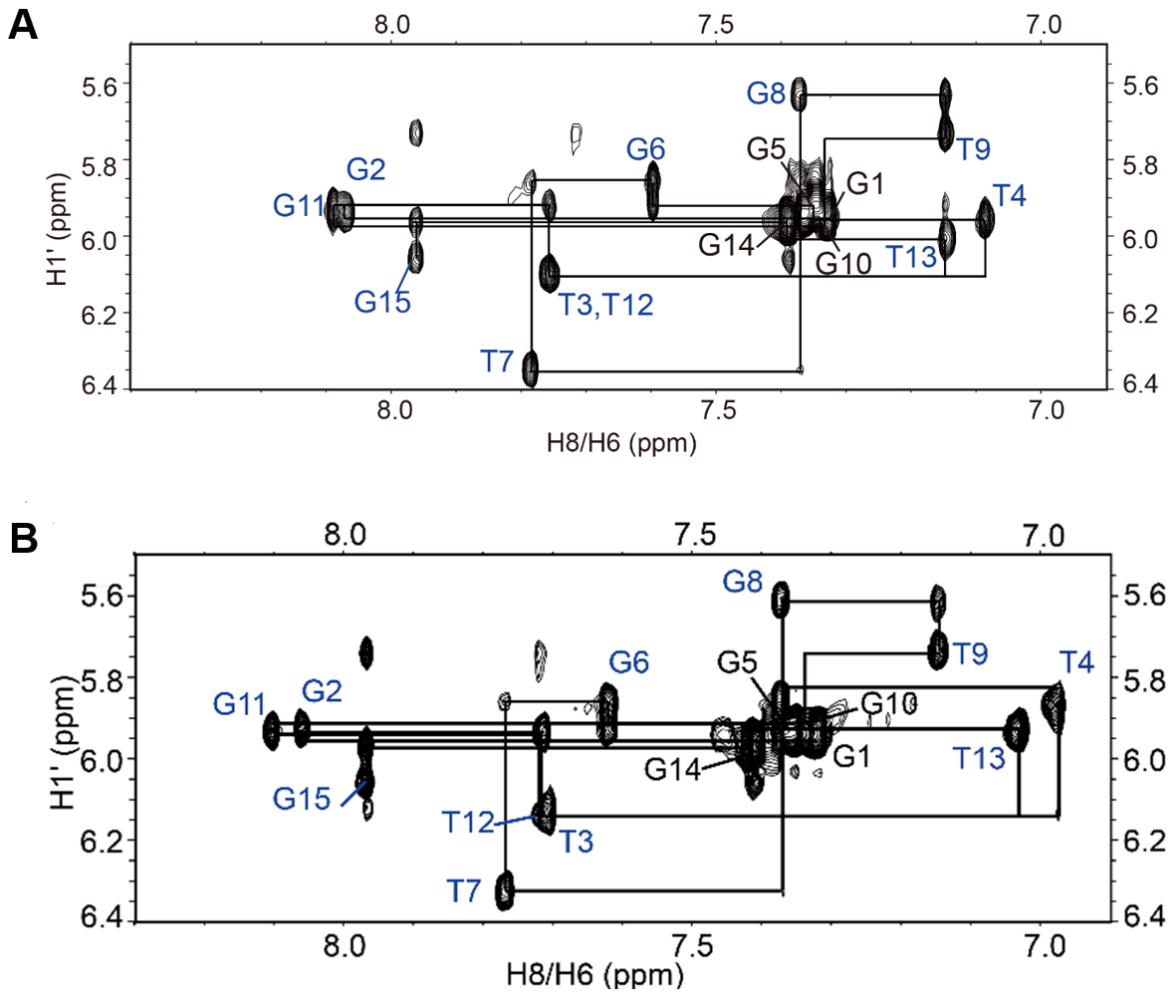

Fig. S13 The H1'-H8/H6 regions of the free TBA G4 (A) and the 1:1 L'$_2$LPt–TBA G4 complex (B) with sequential assignment pathway labelled. Residues with *syn* glycosidic conformations are marked in black, with *anti* glycosidic conformations are marked in blue. Condition: pH 7.0, 25 mM K-phosphate, 70 mM KCl solution, T_m = 25 ℃.

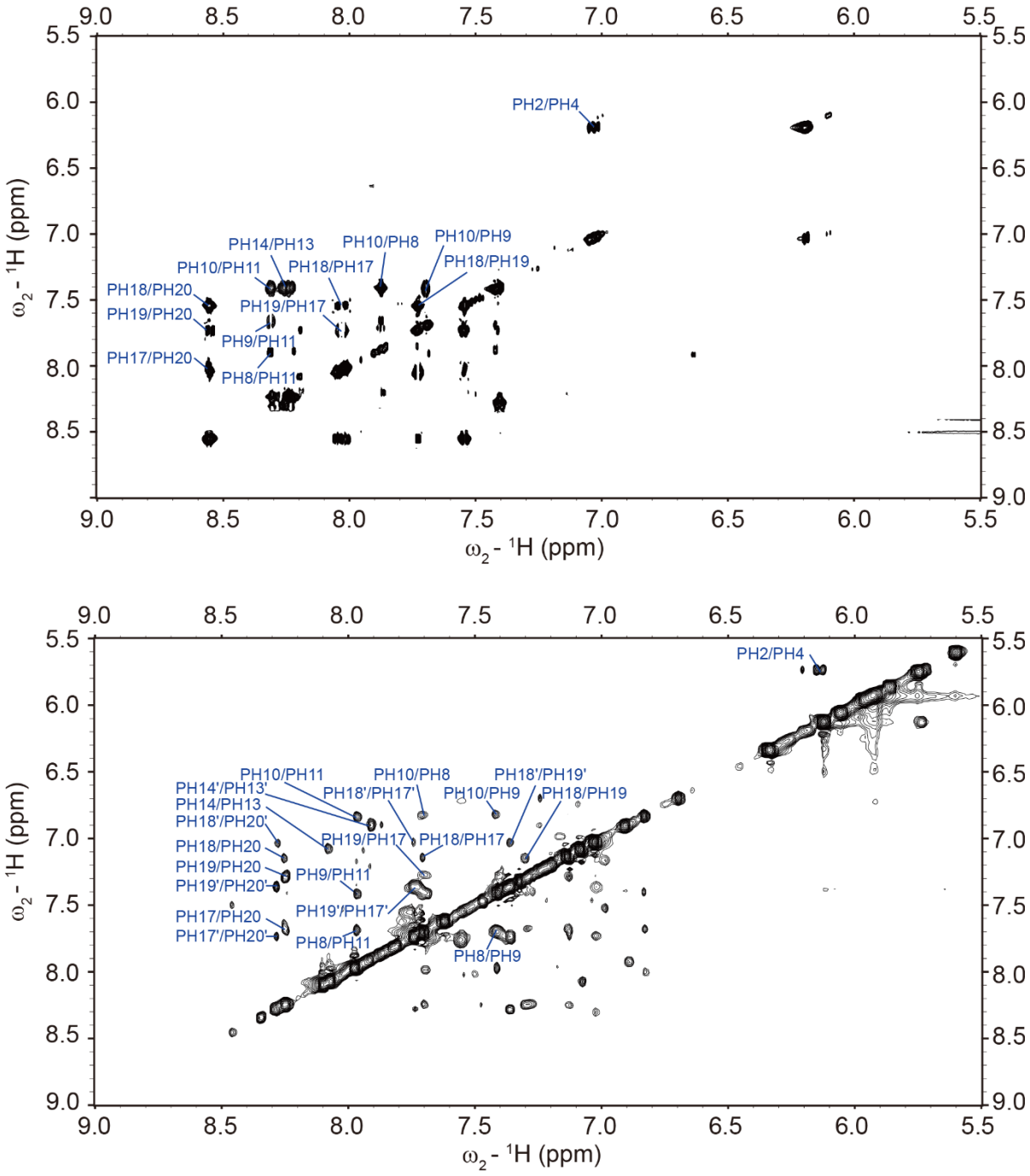

Fig. S14 NMR signal assignments of free L'$_2$LPt (A) and bound L'$_2$LPt (B) at the 1:1 L'$_2$LPt–TBA G4 complex through ^{1}H-^{1}H TOCSY spectra. Condition: pH 7.4, 25 mM K-phosphate, 70 mM KCl solution, T_m = 25 ℃.

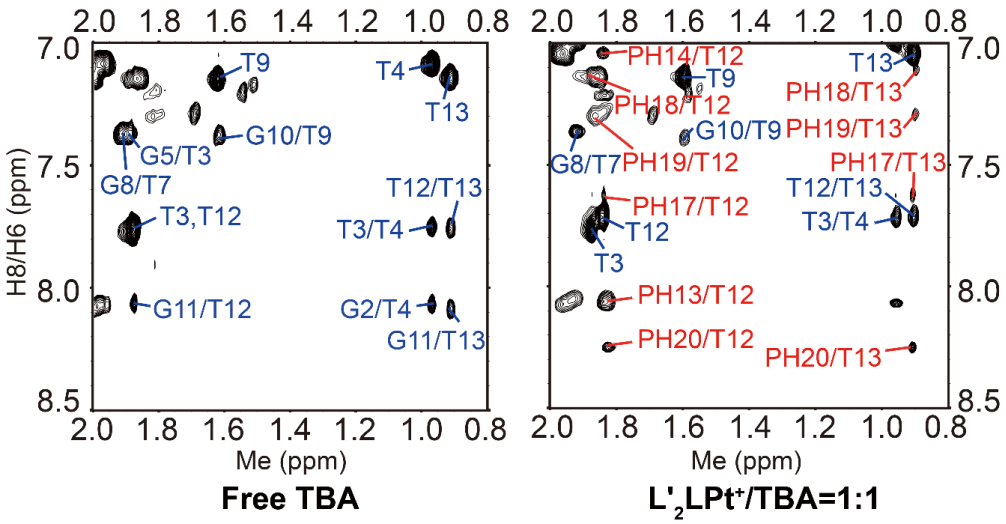

Fig. S15 The NMR NOESY spectra of the free TBA G4 (left) and 1:1 L'$_2$LPt–TBA G4 complex (right). The NOE cross-peaks between L'$_2$LPt and TBA G4 are labeled in red. 'Me' means 'methyl of thymine residue'. Condition: pH 7.4, 25 mM K-phosphate, 70 mM KCl solution, T_m = 25 ℃.

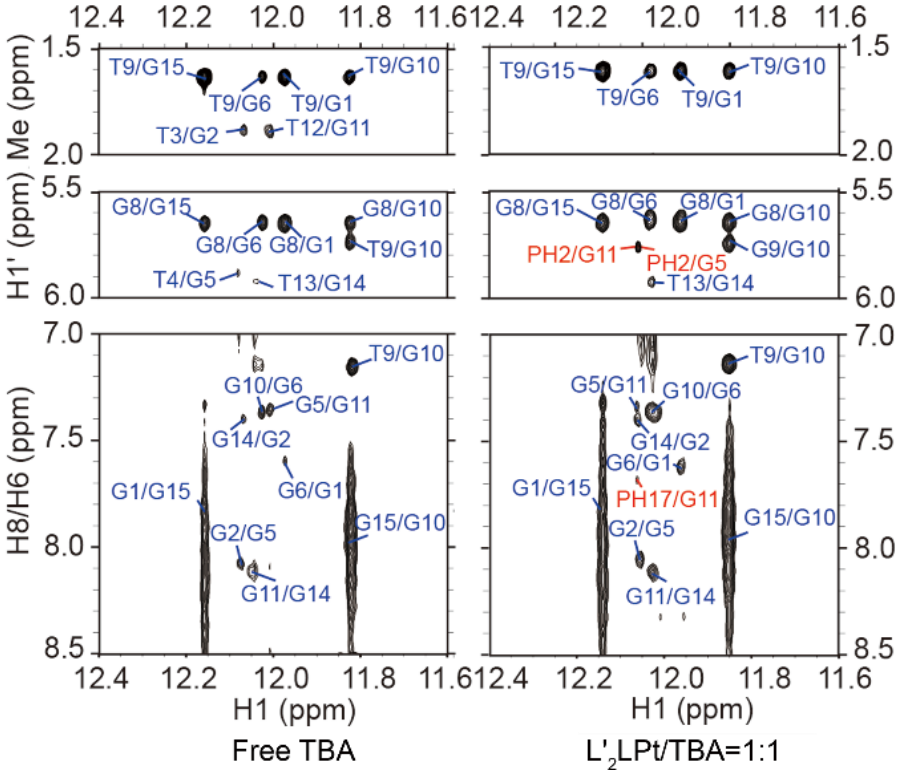

Fig. S16 Expanded H1-H6/H8, H1-H1' and H1-Me regions of 2D NOESY spectrum of free TBA G4 (left) and 1:1 L'$_2$LPt–TBA complex (right). 'Me' means 'methyl of thymine residue'. Inter-molecular cross-peaks between L'$_2$LPt and TBA were labelled in red, and intra-molecular cross-peaks of TBA G4 in both spectrums were labelled in blue. Condition: pH 7.4, 25 mM K-phosphate, 70 mM KCl, 25 ℃.

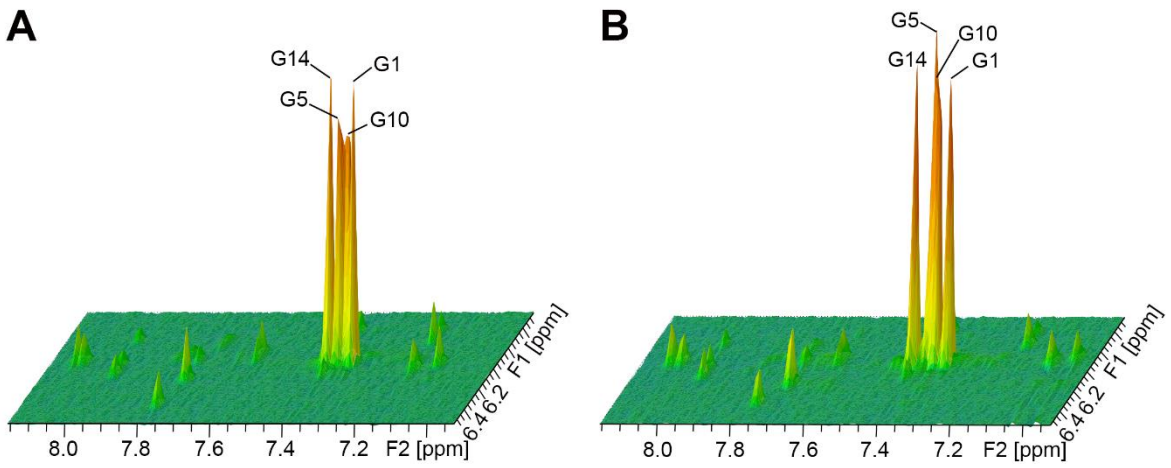

Fig. S17 Stacked plot of the expanded NOESY spectrum (25 ℃) of free TBA (A) and the 1:1 L'$_2$LPt–TBA G4 complex (B). The four strong intra-residue H8-H1' NOEs which correspond to the *syn* glycosidic bonds are labeled with residue number.

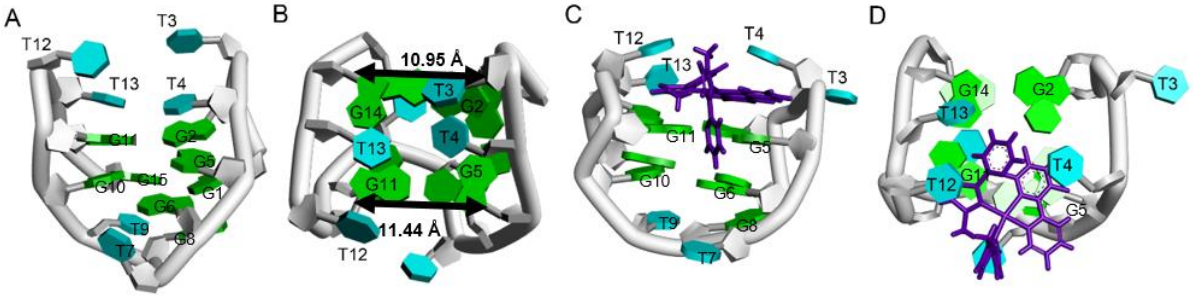

Fig. S18 The structure of free TBA G4 (PDB code: 148D) in (A) side view and (B) top view. And the structure of L'$_2$LPt-TBA complex in (C) side view and (D) top view.

Supplementary Tables

Table S1. Three-dimensional structure of L'_2LPt used in Gaussian 09.

Atom	X	Y	Z	Atom	X	Y	Z
N1	1.8884	0.6436	-2.5011	C17'	-4.0448	0.5768	-2.1975
C1	1.1844	1.0717	-1.4323	C18'	-4.9680	-0.4560	-2.3603
N2	1.3413	2.4445	-1.4525	C29'	-5.1366	-1.3598	-1.3119
C2	2.1464	2.8455	-2.5163	N7	-4.4381	-1.3005	-0.1692
C3	2.4882	1.7116	-3.1682	C20'	-0.1488	0.0355	3.5346
Pt1	-0.0738	0.3896	0.0307	F1	-1.5084	-4.5970	-1.2408
C4	1.5445	-2.1963	0.2079	F2	2.8520	-4.1714	0.4316
C5	2.7317	-1.4133	0.6673	H2	2.3926	3.8732	-2.7217
N3	2.5637	-0.5307	1.6694	H4	3.0961	1.5636	-4.0461
C6	3.6166	0.1935	2.0733	H8	3.4303	0.8889	2.8898
C7	4.8891	0.0871	1.5143	H9	5.7053	0.7005	1.8808
C8	5.0723	-0.8353	0.4838	H10	6.0446	-0.9612	0.0170
C9	3.9863	-1.5959	0.0590	H11	4.1033	-2.3248	-0.7343
C10	0.6364	3.2487	-0.5397	H13	0.8424	-5.4981	-0.4849
C11	0.2951	-1.6079	-0.1437	H14	-1.6845	-2.0630	-0.9269
C12	1.6810	-3.5865	0.0699	H15A	1.5054	5.1473	-1.0914
C13	0.6874	-4.4294	-0.4053	H15B	0.1337	6.4008	0.5602
C14	-0.5084	-3.8227	-0.7597	H15C	-1.4808	5.1338	2.0175
C15	-0.7184	-2.4555	-0.6331	H17	-1.6314	2.6607	1.7517
C16	0.7988	4.6293	-0.4560	H18	1.2827	-1.3520	-2.4513
C17	0.0303	5.3248	0.4730	H19	1.8177	-0.7620	-4.0444
C18	-0.8647	4.6266	1.2850	H20	3.0185	-1.1096	-2.7747
C19	-0.9560	3.2485	1.1427	H13'	-4.5709	-0.8232	2.4330
N4	-0.2215	2.5628	0.2442	H14'	-2.6800	-0.6309	4.4595
C20	2.0114	-0.7368	-2.9706	H15A'	-2.6210	1.4700	-0.8341
N5	-1.3891	-0.1719	2.7854	H15B'	-3.8972	1.3177	-2.9767
C12'	-1.5287	-0.0497	1.4421	H15C'	-5.5522	-0.5540	-3.2685
N6	-2.8622	-0.2967	1.2185	H17'	-5.8570	-2.1703	-1.3889
C13'	-3.5208	-0.5878	2.4113	H18'	0.7009	-0.1007	2.8638
C14'	-2.5951	-0.4979	3.3929	H19'	-0.1368	1.0409	3.9649
C15'	-3.5498	-0.3148	-0.0396	H20'	-0.1010	-0.6974	4.3422
C16'	-3.3227	0.6657	-1.0078				

Table S2. List of DNA sequences used in this research.[11-21]

Type	Name	Sequence
DNA	TBA	5′–GGTTGGTGTGGTTGG–3′
	Tel26	5′–AAAGGGTTAGGGTTAGGGTTAGGGAA–3′
	wtTel26	5′–TTAGGGTTAGGGTTAGGGTTAGGGTT–3′
	wtTel22	5′–AGGGTTAGGGTTAGGGTTAGGG–3′
	c-myc	5′–TGAGGGTGGGTAGGGTGGGTAA–3′
	Bcl2	5′–GGGCGCGGGAGGAATTGGGCGGG–3′
	P1G4T	5′–TGGGCGGGAGCGCGGCGGGCGGGCGGGT–3′
	VEGF	5′–CGGGGCGGGCCTTGGGCGGGGT–3′
	c-kit87up	5′–AGGGAGGGCGCTGGGAGGAGGG–3′
	c-kit*	5′–GGCGAGGAGGGGCGTGGCCGGC–3′
	HIV-PRO1	5′–TGGCCTGGGCGGGACTGGG–3′
	MYT1L	5′–AGGGAGAGGAGAGCTCTGGGTGGGTGGG–3′
	CHL1	5′–GGGTGGGGAAGGGGTGGGT–3′
	ds26	5′–CAATCGGATCGAATTCGATCCGATTG–3′
DNA for FRET	TBA	5′–FAM-GGTTGGTGTGGTTGG-TAMRA–3′
	Tel26	5′–FAM-AAAGGGTTAGGGTTAGGGTTAGGGAA-TAMRA–3′
	wtTel26	5′–FAM-TTAGGGTTAGGGTTAGGGTTAGGGTT-TAMRA–3′
	wtTel22	5′–FAM-AGGGTTAGGGTTAGGGTTAGGG-TAMRA–3′
	c-myc	5′–FAM- TGAGGGTGGGTAGGGTGGGTAA -TAMRA–3′
	Bcl2	5′–FAM-GGGCGCGGGAGGAATTGGGCGGG-TAMRA–3′
	P1G4T	5′–FAM-TGGGCGGGAGCGCGGCGGGCGGGCGGGT-TAMRA–3′
	VEGF	5′–FAM-CGGGGCGGGCCTTGGGCGGGGT-TAMRA–3′
	c-kit87up	5′–FAM-AGGGAGGGCGCTGGGAGGAGGG-TAMRA–3′
	c-kit*	5′–FAM-GGCGAGGAGGGGCGTGGCCGGC -TAMRA–3′
	HIV-PRO1	5′–FAM-TGGCCTGGGCGGGACTGGG-TAMRA–3′
	MYT1L	5′–FAM-AGGGAGAGGAGAGCTCTGGGTGGGTGGG-TAMRA–3′
	CHL1	5′–FAM-GGGTGGGGAAGGGGTGGGT-TAMRA–3′
	F10T	5′–FAM-CAATCGGATCGAA-HEG-TTCGATCCGATTG-TAMRA–3′

Table S3. Stabilization temperature ΔT_m (°C) of L'$_2$LPt binding to different G4 (Tel26, wtTel26, wtTel22, c-myc, Bcl2, P1G4T, VEGF, c-kit87up, c-kit*, HIV-PRO1, MYT1L, CHL1 and TBA) and dsDNA (F10T) in FRET assay.

DNA	Tel26	wtTel26	wtTel22	c-myc	Bcl2	P1G4T	VEGF
ΔT_m (°C)	5.4 ±0.4	4.7 ±0.2	3.2 ±0.4	3.0 ±0.2	2.1 ±0.3	1.3 ±0.2	1.3 ±0.1
DNA	c-kit87up	MYT1L	CHL1	c-kit*	HIV-PRO1	TBA	F10T
ΔT_m (°C)	2.8 ±0.3	0.6 ±0.1	0.2 ±0.0	1.4 ±0.2	6.4 ±0.4	12.4 ±0.3	0.0 ±0.0

Table S4. Melting temperature ΔT_m (°C) of L'$_2$LPt binding to different G4s (Tel26, wtTel26, wtTel22, c-myc, Bcl2, P1G4T, VEGF, c-kit87up, c-kit*, HIV-PRO1, MYT1L, CHL1 and TBA) and ds26 in CD-melting assay.

DNA	Tel26	wtTel26	wtTel22	c-myc	Bcl2	P1G4T	VEGF
ΔT_m (°C)	5.8 ±0.2	6.7 ±0.3	4.0 ±0.5	4.2 ±0.4	2.6 ±0.2	1.8 ±0.4	1.1 ±0.2
DNA	c-kit87up	MYT1L	CHL1	c-kit*	HIV-PRO1	TBA	ds26
ΔT_m (°C)	2.0 ±0.3	0.2 ±0.1	0.9 ±0.3	7.6 ±0.3	7.8 ±0.8	16.4 ±0.5	0.2 ±0.1

Table S5. The concentration of K^+ used for each G4s (Tel26, wtTel26, wtTel22, c-myc, Bcl2, P1G4T, VEGF, c-kit87up, c-kit*, HIV-PRO1, MYT1L, CHL1 and TBA) and ds26 in FRET assay.

DNA	Tel26	wtTel26	wtTel22	c-myc	Bcl2	P1G4T	VEGF
K^+ (mM)	500	500	500	2	10	2	0.5
DNA	c-kit87up	MYT1L	CHL1	c-kit*	HIV-PRO1	TBA	ds26
K^+ (mM)	100	100	0.5	200	100	200	100

Table S6. Melting temperature ΔT_m (°C) of L'$_2$LPt binding to different G4s (Tel26, wtTel26, wtTel22, c-myc, Bcl2, P1G4T, VEGF, c-kit87up, c-kit*, HIV-PRO1, MYT1L, CHL1 and TBA) and ds26 in FRET assay.

DNA	Tel26	wtTel26	wtTel22	c-myc	Bcl2	P1G4T	VEGF
ΔT_m (°C)	4.0 ±0.4	3.5 ±0.3	3.7 ±0.4	2.2 ±0.4	0.3 ±0.1	0.8 ±0.2	-0.1 ±0.2
DNA	c-kit87up	MYT1L	CHL1	c-kit*	HIV-PRO1	TBA	ds26
ΔT_m (°C)	1.0 ±0.3	0.1 ±0.1	0.4 ±0.1	0.6 ±0.2	7.3 ±0.2	15.2 ±0.7	0.2 ±0.1

Table S7. FRET competition experiments with different ratios (1:0, 1:1, 1:15, 1:50) of duplex-DNA and G4 (ds26, VEGF, Tel26, HIV-PRO1) added to TBA. Conditions:10 mM Tris-HCl buffer containing 60 mM potassium cacodylate, pH = 7.4.

	DS26	**VEGF**	**Tel26**	**HIV-PRO1**
1:0	100	100	100	100
1:1	97.1 ±0.93	95.7 ±1.09	81.6 ±1.86	62.1 ±3.03
1:15	90.3 ±1.28	84.1 ±1.15	40.1 ±1.87	17.2 ±0.92
1:50	75.8 ±1.80	58.4 ±2.73	17.2 ±2.34	6.29 ±0.91

Table S8. ^{1}H NMR chemical shifts (ppm) of the free TBA and free L'$_2$LPt at 25 ℃.

TBA G4	H6/H8	Me/H5/H1	H1'	H2'	H2''	H3'	H4'	H5'	H5''
C1	7.33	11.95	5.96	2.87	2.87	4.9	4.31	4.16	4.01
G2	8.07	12.05	5.92	2.26	2.89	5.05	4.31	4.18	4.01
G3	7.76	1.88	6.1	2.1	2.46	4.8	4.3	4.21	3.83
G4	7.08	0.97	5.96	1.96	2.54	4.81	4.19	4.09	3.82
G5	7.35	12.07	5.91	2.77	3.31	4.77	4.34	4.16	4.15
C6	7.6	12.03	5.85	2.67	3.3	5.02	4.34	4.16	3.9
G7	7.78	1.88	6.35	2.39	2.51	4.72	4.34	4.14	3.96
G8	7.37	10.48	5.63	2.78	3.3	4.73	4.1	3.91	3.59
G9	7.15	1.62	5.73	2.26	2.92	4.53	3.82	3.62	3.46
C10	7.34	11.83	5.94	2.81	3.59	4.8	4.31	4.18	4.17
C11	8.08	11.98	5.94	2.24	2.86	5.04	4.29	4.2	3.57
T12	7.76	1.88	6.1	2.1	2.46	4.81	4.2	4.13	3.83
T13	7.15	0.91	6.01	2.46	2.61	4.81	4.3	4.21	3.83
G14	7.33	12.04	5.96	2.87	2.87	4.9	4.31	4.16	4.01
G15	8.07	12.15	5.92	2.26	2.89	5.05	4.31	4.18	4.01

L'$_2$LPt	**H2**	**H4**	**H8**	**H9**	**H10**	**H11**	
	6.19	7.03	7.87	7.69	7.42	8.03	
	H13/H13'	**H14/H14'**	**Me15/Me15'**	**H17/H17'**	**H18/H18'**	**H19/H19'**	**H20/H20'**
	8.23	7.40	3.01/3.06	8.03	7.54	7.73	8.55

Table S9. ^{1}H NMR chemical shifts (ppm) of the 1:1 L'$_2$LPt-TBA complex at 25 ℃.

TBA G4	H6/H8	Me/H5/H1	H1'	H2'	H2''	H3'	H4'	H5'	H5''
C1	7.33	11.96	5.96	2.87	2.87	4.9	4.31	4.16	4.01
G2	8.07	12.06	5.92	2.26	2.89	5.06	4.31	4.18	4.01
G3	7.76	1.88	6.13	2.07	2.43	4.8	4.31	4.15	3.77
G4	6.98	0.94	5.87	1.93	2.51	4.81	4.19	4.06	3.77
G5	7.38	12.06	5.93	2.77	3.31	4.77	4.34	4.16	4.15
C6	7.61	12.04	5.85	2.67	3.3	5.02	4.34	4.16	3.9
G7	7.78	1.88	6.35	2.39	2.51	4.72	4.34	4.14	3.96
G8	7.37	10.48	5.63	2.78	3.3	4.73	4.1	3.91	3.59
G9	7.15	1.62	5.73	2.26	2.92	4.53	3.82	3.62	3.46
C10	7.34	11.87	5.9	2.81	3.59	4.8	4.31	4.18	4.17
C11	8.1	12.06	5.99	2.24	2.86	5.08	4.29	4.18	3.53
T12	7.73	1.88	6.13	2.07	2.43	4.81	4.31	4.18	3.77
T13	7.04	0.89	5.89	2.44	2.56	4.79	4.3	4.21	3.76
G14	7.39	12.04	5.96	2.8	3.43	4.83	4.32	4.15	4.13
G15	7.96	12.14	6.06	2.6	2.34	4.84	4.27	4.16	4.08

L'$_2$LPt	**H2**	**H4**	**H8**	**H9**	**H10**	**H11**	
	5.75	6.14	7.69	7.41	6.84	7.97	
	H13	**H14**	**Me15**	**H17**	**H18**	**H19**	**H20**
	8.08	7.07	3.03	7.68	7.14	7.29	8.25
	H13'	**H14'**	**Me15'**	**H17'**	**H18'**	**H19'**	**H20'**
	7.92	6.90	3.03	7.73	7.03	7.36	8.28

Table S10. Observed intermolecular NOE cross-peaks of the L'$_2$LPt and the G-tetrad of TBA. The intensity of the NOE peaks is showed by 'S' (strong), 'M' (medium) or 'W' (weak), respectively.

		L'$_2$LPt												
		H2	**H4**	**H8**	**H9**	**H10**	**H11**	**H13**	**H14**	**H15**	**H17**	**H18**	**H19**	**H20**
G5	**H1**	M	M											
	H8	W	M	W	W	W	W						W	W
	H1'		W	M	W									
	H2'													
	H2''													
	H3'													
	H4'				W	W								
	H5'													
	H5''													
G11	**H1**	M						W	W		M			
	H8							M	W	W	W			
	H1'							W	M	S		W		W
	H2'							M	S	S				
	H2''							S	M	S				
	H3'									M				
	H4'													
	H5'													
	H5''													

Table S11. Observed intermolecular NOE cross-peaks of the L'$_2$LPt and the flanking/loop of TBA. The intensity of the NOE peaks is showed by 'S' (strong), 'M' (medium) or 'W' (weak), respectively.

	L'$_2$LPt$^+$													
		H10	**H8**	**H4**	**H3**	**H2**	**H1**	**H14**	**H13**	**H15**	**H17**	**H18**	**H19**	**H20**
T4	**Me**		M										S	S
	H6		M										W	W
	H1'		M	W										
	H2'		M	W										
	H2''		M	W										
	H3'		W											
	H4'													
	H5'													
	H5''													
T12	**Me**							S	S	W	W	M	M	M
	H6							M	S	W	W			
	H1'							M	W	S				
	H2'							S	M	W				
	H2''							S	M	W				
	H3'													
	H4'													
	H5'													
	H5''													
T13	**Me**										M	M	W	W
	H6								W		W			
	H1'													
	H2'								W		W	W		
	H2''													
	H3'													
	H4'													
	H5'													
	H5''													

Table S12. Structural statistics for the solution structure of the 1:1 complex of L'$_2$LPt and TBA G4.

Structural Statistics	
NMR distance and dihedral constraints	
Distance restraints	
Total NOE	312
Intra-residue	95
Inter-residue	118
Hydrogen bond	16
L'$_2$LPt	
Intramolecular	6
Intermolecular (L'$_2$LPt / TBA G4)	77
Total dihedral angle restraints	8
Structure statistics	
Violations (mean and s.d.)	
Distance constraints (Å)	0.038 ± 0.014
Dihedral angle constraints (°)	0.898 ± 0.203
Max. dihedral angle violation (°)	11.01
Max. distance constraint violation (Å)	0.207
Deviations from standard geometry	
Bond length (Å)	0.026 ± 0.011
Bond angle (°)	1.502 ± 0.012
Impropers (°)	0.934 ± 0.019
Average pairwise r.m.s.d of heavy atoms (Å)	
G-tetrad	1.26 ± 0.24
All	2.45 ± 0.52

Table S13. Fibrinogen clotting time of thrombin alone (1.0 ml of PBS containing 2.0 mg/ml of fibrinogen added with 100µl/10 NIH per ml of human thrombin) or in the presence of 0, 200, 500 and 1000 nM concentrations of TBA, 1.0 equivalent of other TBA binders (TMPyP$_4$ and PDS) and different equivalents of L'$_2$LPt. The bars of control and vehicle represent the fibrinogen clotting time values of the system in absence of any L'$_2$LPt/TBA and diluted with the buffer alone, respectively.

	0 nM	**200 nM** (s)	**500 nM** (s)	**1000 nM** (s)
CONTROL	15.5 ± 0.2	15.5 ± 0.2	15.3 ± 0.2	15.4 ± 0.1
VEHICLE	15.7 ± 0.2	15.6 ± 0.2	15.7 ± 0.2	15.5 ± 0.2
TBA	15.6 ± 0.3	52.7 ± 2.3	97.4 ± 2.4	133.8 ± 3.1
TBA+1.0eq. TMPyP4	15.9 ± 0.1	47.8 ± 1.3	85.5 ± 0.8	118.6 ± 1.5
TBA+1.0eq. PDS	15.8 ± 0.3	45.1 ± 2.0	79.5 ± 3.7	111.9 ± 3.3
TBA+1.0eq. L'$_2$LPt	16.9 ± 0.5	43.9 ± 1.7	75.2 ± 1.8	108.2 ± 2.4
TBA+2.0eq. L'$_2$LPt	17.4 ± 0.4	36.5 ± 1.7	51.9 ± 3.4	74.7 ± 4.1
TBA+3.0eq. L'$_2$LPt	19.1 ± 0.8	29.3 ± 0.9	38.8 ± 3.0	55.6 ± 3.9

References

1. R. Thenarukandiyil and J. Choudhury, *Organometallics*, 2015, **34**, 150506131023005.
2. J.-J. Zhong, C. Yang, X.-Y. Chang, C. Zou, W. Lu and C.-M. Che, *Chem. Comm.*, 2017, **53**, 8948-8951.
3. A. Marchand, D. Strzelecka and V. Gabelica, *Chem. Eur. J.*, 2016, **22**, 9551-9555.
4. V. Gabelica, R. Maeda, T. Fujimoto, H. Yaku, T. Murashima, N. Sugimoto and D. Miyoshi, *Biochem.*, 2013, **52**, 5620-5628.
5. P. Kuzmic, *Anal. Biochem.*, 1996, **237**, 260-273.
6. A. Pica, I. Russo Krauss, V. Parente, H. Tateishi-Karimata, S. Nagatoishi, K. Tsumoto, N. Sugimoto and F. Sica, *Nucleic Acids Res.*, 2016, **45**, 461-469.
7. N. A. Treuheit, M. A. Beach and E. A. Komives, *Biochem.*, 2011, **50**, 4590-4596.
8. W. Liu, Y.-F. Zhong, L.-Y. Liu, C.-T. Shen, W. Zeng, F. Wang, D. Yang and Z.-W. Mao, *Nat. Comm.*, 2018, **9**, 3496.
9. A. Brünger, 1993.
10. M. Scuotto, E. Rivieccio, A. Varone, D. Corda, M. Bucci, V. Vellecco, G. Cirino, A. Virgilio, V. Esposito, A. Galeone, N. Borbone, M. Varra and L. Mayol, *Nucleic Acids Res.*, 2015, **43**, 7702-7716.
11. P. Schultze, R. F. Macaya and J. Feigon, *J. Mol. Biol.*, 1994, **235**, 1532-1547.
12. J. Dai, C. Punchihewa, A. Ambrus, D. Chen, R. A. Jones and D. Yang, *Nucleic Acids Res.*, 2007, **35**, 2440-2450.
13. J. Dai, M. Carver, C. Punchihewa, R. A. Jones and D. Yang, *Nucleic Acids Res.*, 2007, **35**, 4927-4940.
14. J. Dai, M. Carver, L. H. Hurley and D. Yang, *J. Am. Chem. Soc.*, 2011, **133**, 17673-17680.
15. B. Onel, M. Carver, G. Wu, D. Timonina, S. Kalarn, M. Larriva and D. Yang, *J. Am. Chem. Soc.*, 2016, **138**, 2563-2570.
16. P. Agrawal, E. Hatzakis, K. Guo, M. Carver and D. Yang, *Nucleic Acids Res.*, 2013, **41**, 10584-10592.
17. A. T. Phan, V. Kuryavyi, S. Burge, S. Neidle and D. J. Patel, *J. Am. Chem. Soc.*, 2007, **129**, 4386-4392.
18. A. Kotar, R. Rigo, C. Sissi and J. Plavec, *Nucleic Acids Res.*, 2018, **47**, 2641-2653.
19. S. Amrane, A. Kerkour, A. Bedrat, B. Vialet, M.-L. Andreola and J.-L. Mergny, *J. Am. Chem. Soc.*, 2014, **136**, 5249-5252.
20. K. W. Lim, P. Jenjaroenpun, Z. J. Low, Z. J. Khong, Y. S. Ng, V. A. Kuznetsov and A. T. Phan, *Nucleic Acids Res.*, 2015, **43**, 5630-5646.
21. V. Kuryavyi and D. J. Patel, *Structure*, 2010, **18**, 73-82.